Arithmetic with q-plates

SAM DELANEY[1], MARÍA M. SÁNCHEZ-LÓPEZ[2,*], IGNACIO MORENO[3] AND JEFFREY A. DAVIS[1]

[1]*Department of Physics. San Diego State University, San Diego, CA 92182-1233, USA*
[2]*Instituto de Bioingeniería. Dept. Física y Arquitectura de Computadores, Universidad Miguel Hernández, 03202 Elche, Spain*
[3]*Departamento de Ciencia de Materiales, Óptica y Tecnología Electrónica. Universidad Miguel Hernández, 03202 Elche, Spain*
**Corresponding author: mar.sanchez@umh.es*

Received XX Month XXXX; revised XX Month, XXXX; accepted XX Month XXXX; posted XX Month XXXX (Doc. ID XXXXX); published XX Month XXXX

In this work we show the capability to form various *q*-plate equivalent systems using combinations of commercially available *q*-plates. We show operations like changing the sign of the *q*-value, or the addition and subtraction of *q*-plates. These operations only require simple combinations of *q*-plates and half-wave plates. Experimental results are presented in all cases. Following this procedure, experimental testing of higher and negative q-valued devices can be carried out using commonly available q-valued devices. © 2016 Optical Society of America

OCIS codes: *(230.3720) Liquid-crystal devices, (230.5440) Polarization-selective devices, (120.5410) Polarimetry.*

http://dx.doi.org/10.1364/AO.99.099999

1. INTRODUCTION

Optical retarder elements with azimuthal rotation of the principal axes are receiving a great deal of attention because they can create cylindrically polarized vector beams, and can transfer orbital angular momentum (OAM) to light [1]. Both OAM and vector beam multiplexing are under investigation for optical communication applications [2-5]. Radially and azimuthally polarized beams, which are the most common versions of vector beams [6,7] have attracted much attention for their sharper focusing [8,9]. Furthermore, because of their axial electric and magnetic field distribution, they find also interesting applications in optical tweezing [10], materials processing [11] or super-resolution microscopy [12].

These cylindrically polarized beams can be generated using *q*-plates which are half-wave retarders where the principal axis rotates with the azimuth angle. These devices can be fabricated with special liquid crystal patterns [13-17], or by means of local polarization transformation of metasurfaces [18-20].

In all cases, the *q*-plate value is fixed in the fabrication process. Therefore, if the *q*-value must be changed, another *q*-plate is required. In Ref. [21] we demonstrated a system where the *q*-value is doubled by using a reflective geometry where light passes twice through the device. A quarter-wave plate (QWP) was required in between the *q*-plate and the mirror to yield this doubling *q*-value effect. Another option employs an SLM to encode *q*-plates. In this case any *q*-value can be programmed. However, this requires an expensive pixelated device, and an optical architecture to modulate the two electric field components [22,23].

Commercial *q*-plates are now available with typical *q*-values of $q=1/2$ and $q=1$. Therefore, it is interesting to investigate whether these *q*-plates can be combined in order to generate equivalent devices of different *q*-values to allow experimentation before purchasing the target devices. For example, two metasurface *q*-plate elements were combined in [24]. The addition and subtraction of OAM was shown for input circularly polarized light. This mechanism was then applied in a system using two *q*-plates [25], or an SLM and a *q*-plate [26], to generate a vector vortex beam, i.e. a vector beam that exhibits different topological charge in the two circular polarization components. The first *q*-plate was used to generate a scalar vortex beam, which then illuminates a second *q*-plate. The resulting vector vortex beam is different of the usual pure vector beams generated with a *q*-plate illuminated with a homogenous polarization, that shows the same charge but with opposite sign in the two circular polarization components.

In this work we analyze the general performance of *q*-plate devices placed in cascade, and show their arithmetic properties. We use the Jones matrix formalism to demonstrate that the sign of the *q*-plate can be reversed simply by placing the *q*-plate in between two half-wave plates (HWP). Then we extend the study in [24] by showing that a system composed of two *q*-plates in cascade followed by a half-wave retarder (HWP) is equivalent to an effective *q*-plate device where the *q* values subtract. Instead, if the HWP is placed in between the two *q*-plates, then the *q*-values add. With this scheme for obtaining equivalent *q*-plate systems with reduced or enhanced *q* values, not only the subtraction and summation of OAM is achieved, but we can generate all the vector beams corresponding to the effective charge *q*. We use these properties to build different *q*-plate systems with *q* values ranging from +2.5 to -2.5 in steps of 0.5, using just three individual *q*-plates. The experimental results validate the theory.

The paper is organized as follows. After this introduction, Section 2 briefly reviews the *q*-plate device and its operation. In Section 3 we

mathematically demonstrate useful decompositions of the q-plate matrix to perform sign inversion, addition and subtraction of q-values, and experimentally validate them. Then, in section 4 the above-mentioned properties are applied to obtain effective q-plate systems of ten different q-values using only three devices. Finally, Section 5 contains the conclusions of our work.

2. REVIEW OF THE Q-PLATE OPERATION

The q-plate consists of a linear phase plate retarder with a retardance of π radians where the principal axis of the retarder follows q times the azimuthal angle θ. The Jones matrix for this device is given by [13]:

$$\mathbf{M}(q)=\begin{pmatrix}\cos(2q\theta) & \sin(2q\theta)\\ \sin(2q\theta) & -\cos(2q\theta)\end{pmatrix}. \qquad (1)$$

These q-plates are sometimes defined by the topological charge that they add to the light beam, $\ell=2q$, instead of by their order q; we will use both notations in this work.

The experimental system is similar to the system we used for a single q-plate [27]. Light from a He-Ne laser was spatially filtered and collimated. To generate and detect linearly or circularly polarized light, we used high quality linear polarizers and wave plates from Meadowlark Optics. We used commercially available q-plates from Thorlabs, identified as vortex half-wave plates. We use two plates with q=1 and one with q=1/2. To verify the circular polarization states, we used two R and L circular polarizer sheets from Aflash Photonics. The transmitted light was sent to a camera.

Figure 1 gives a quick review of the characteristic properties of the q-plate where q=1/2 when illuminated and analyzed with a limited number of polarization states. More extensive results are given in [27]. Figures 1(b), 1(c) and 1(d) show the experimental results obtained when the q-plate is illuminated with linearly polarized light vertically oriented, oriented at 45º, and with right circular polarization, respectively. For each case, we capture the beam without analyzer (No Ana), and by adding a linear analyzer that is oriented vertically, at 45º, horizontally, at 135º, and with left circular polarization (LCP) and right circular polarization (RCP) analyzers. Note that these six images can be used directly to calculate the corresponding Stokes parameters images, as presented for instance in Ref. [20].

In order to better understand the images, the polarization pattern is drawn superimposed to the image without analyzer. When illuminated with vertically polarized light, the output is radially polarized (Fig 1(b)). This is shown by the bright areas that appear when the linear polarizer is used as analyzer. Note how they are aligned with the analyzer's orientation. If the incident light is rotated by 45 degrees, then we see that the bright areas rotate in the same direction as the analyzer (Fig. 1(c)). Finally, when illuminated with RCP, the beam shows uniform intensity for all orientations of the linear analyzer, while maximum brightness is observed for the LCP analyzer and total extinction occurs when using the RCP analyzer. This confirms that under RCP illumination the output becomes LCP with an azimuthal phase of $\ell=2q$. This azimuthal phase is seen as a vortex dark spot in the center of the pattern. However, in Fig. 1(d) it is too small to be resolved.

Similar results are obtained with higher order q-plate values [27]. Next, we examine useful decompositions of the q-plate matrix representation that allow us to obtain addition and subtraction arithmetic effects.

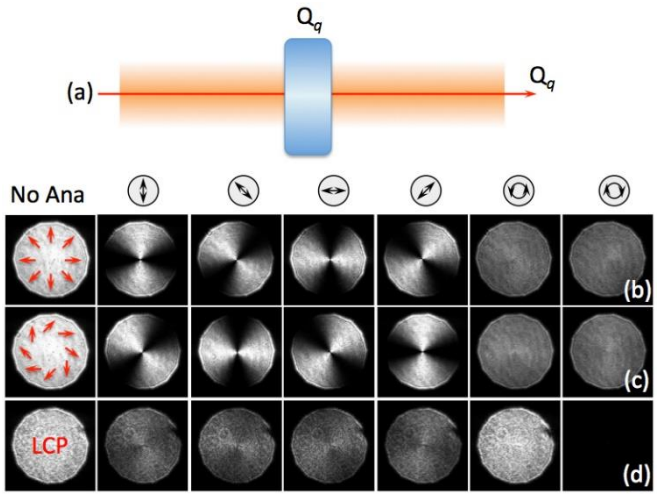

Fig. 1. Scheme for a single q-plate (a) and resulting experimental polarization patterns for q=1/2. The device transforms (b) vertical linear polarization into radial polarization, (c) linearly polarized light at 45º into slanted polarization, and (d) RCP into LCP plus an azimuthal phase.

3. DECOMPOSITION OF Q-PLATES

The q-plate matrix of Eq. (1) can be decomposed in two ways:

$$\mathbf{M}(q)=\mathbf{HWP}\cdot\mathbf{R}(+2q\theta)=\mathbf{R}(-2q\theta)\cdot\mathbf{HWP}, \qquad (2)$$

where

$$\mathbf{HWP}=\begin{pmatrix}1 & 0\\ 0 & -1\end{pmatrix},\quad \mathbf{R}(\theta)=\begin{pmatrix}\cos(\theta) & \sin(\theta)\\ -\sin(\theta) & \cos(\theta)\end{pmatrix} \qquad (3)$$

are, respectively, the Jones matrix for an aligned half-wave plate (HWP) and the rotation matrix. We follow the convention in Ref. [28] for Jones matrices.

Note the two different Jones matrix decompositions in Eq. (2). In the first case, light goes first through the positive rotation matrix and then passes through the aligned HWP. Alternatively, the q-plate matrix is decomposed as first a HWP followed by a negative rotation matrix.

3.1. Changing the sign of the q-plate

A positive q-plate can be converted to a negative q-plate simply by placing a HWP on both sides as shown in Fig. 2(a).

Using the first decomposition of Eq. (2), this would be written as

$$\mathbf{M}(-q)=\mathbf{HWP}\cdot\mathbf{R}(-2q\theta)=\mathbf{HWP}\cdot\mathbf{M}(-q)\cdot\mathbf{HWP} \qquad (4)$$

where we used that the product of two HWPs is the identity matrix.

Figure 2 shows experimental results corresponding to this situation, where again we consider the q-plate with q=1/2. The major difference when comparing to Fig. 1 occurs when the q-plate system is illuminated with linear vertical polarization, and we analyze the vector beam with the linear polarizer oriented at ±45 degrees. In Fig. 1, the bright areas rotate in the same sense as the linear analyzer rotates (counterclockwise). However, for the negative q-plate, the bright areas rotate clockwise. This agrees with the expected polarization patterns, which once again are superimposed on the images captured without analyzer. Note too that the light emerging from the system is again LCP when illuminated with RCP (Fig. 2(d)), as it is expected for a q-plate device.

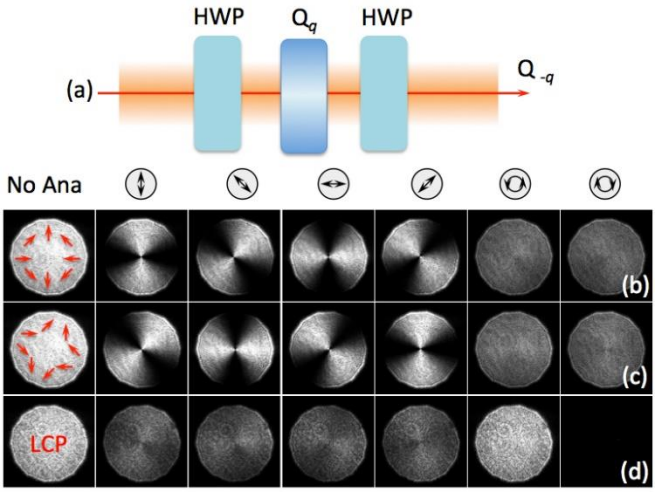

Fig. 2. Scheme for the system changing the sign of a q-plate (a) and experimental polarization patterns for q=–1/2 when illuminated with: (b) vertical linear polarization, (c) linearly polarized light at 45º, and (d) RCP.

3.2. Adding two q-plates

We can add two q-plates simply by inserting a HWP between them as shown in Fig. 3. In this case, the system would be represented as in Eq. (5):

$$\begin{aligned}\mathbf{M}(q_1+q_2) &= \mathbf{HWP}\cdot\mathbf{R}(2[q_1+q_2]\theta) = \\ &= \mathbf{HWP}\cdot\mathbf{R}(2q_2\theta)\cdot\mathbf{R}(2q_1\theta) = \\ &= \mathbf{M}(q_2)\cdot\mathbf{HWP}\cdot\mathbf{M}(q_1)\end{aligned} \qquad \textbf{(5)}$$

where again we used Eq. (2), the fact that two consecutive rotation matrices are equivalent to a single rotation of the added rotation angles, and the property that two HWPs give the identity matrix. Note that the approach used in Ref. [21] to double the charge of a q-plate in a reflective geometry essentially implements the system in Eq. (5), but using a quarter-wave plate in reflection to act as a HWP.

Experimental results for this system are shown in Figs. 3(b) and 3(c). The first case corresponds to the addition of two q-plates with values of q=1/2 and q=1, while the second case shows the addition of two q-plates having both values of q=1. Therefore, the resulting q-plate systems have q-values q=3/2 and q=2 respectively. For simplicity we only show the results when the incident polarization is vertical.

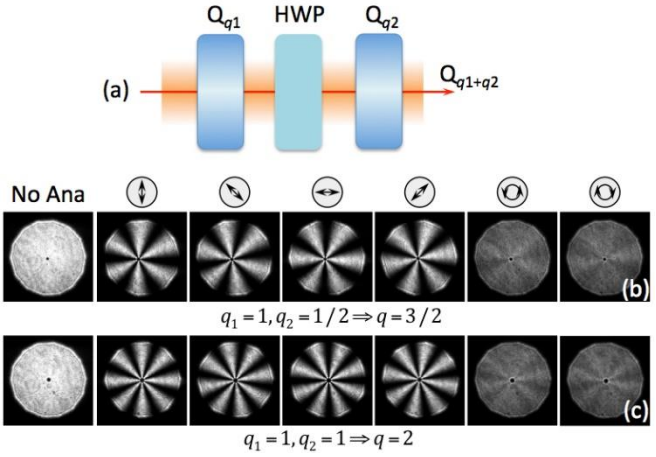

Fig. 3. System for adding two q-plates (a) and resulting experimental polarization patterns when illuminated with vertical linear polarization: (b) Addition of q=1 and q=1/2, (c) Addition of two q-plates with q=1.

We see two effects. First, the singularity in the center becomes larger as the sum of topological charges in the emerging beams increases from $\ell=3$ to $\ell=4$, where $\ell=2(q_1+q_2)$. This was basically not observed in prior examples in Figs. 1 and 2 because the resolution of the camera was too small. And more evidently, when viewed between two linear polarizers, we now see 6 and 8 bright areas, respectively, corresponding to 2ℓ. Finally, also note that, since the two added q-plates are positive, the resulting q-plate is also positive, as it can be verified by following the rotation of the bright areas in Figs. 3(b) and 3(c), which rotate in the same sense as the linear analyzer does.

3.3. Subtracting two q-plates

We can subtract two q-plates by inserting a HWP after them as shown in Fig. 4(a). In this case, the system would be represented as:

$$\begin{aligned}\mathbf{M}(q_1-q_2) &= \mathbf{HWP}\cdot\mathbf{R}(2[q_1-q_2]\theta) = \\ &= \mathbf{HWP}\cdot\mathbf{R}(-2q_2\theta)\cdot\mathbf{R}(+2q_1\theta) = \\ &= \mathbf{HWP}\cdot\mathbf{M}(q_2)\cdot\mathbf{M}(q_1)\end{aligned} \qquad \textbf{(6)}$$

where we used the properties in Eq. (2) and (4).

The corresponding experimental results are shown in Figs. 4(b) to 4(d) for two cases. First, when the two q-plates have identical values, they subtract yielding a zero polarization distribution (Fig. 4(b)). In this case we used the two q-plates with q=1. As a result there is no modification in the state of polarization, which remains homogeneously linearly polarized along the vertical direction. Note that the singularity is clearly visible. This can be caused either if the two q-plates are not exactly centered or if they are too far apart. In the latter case, the Fresnel diffraction from the first might be larger than the second. The singularity can be reduced with more perfect alignment, but we feel it is adequately small in these images.

In the second case we use q=1/2 and q=1. This situation shows the importance of the order in which the devices are placed. In Fig. 4(c), the plate with q=1 is placed first, so the resulting q-plate system has value q=+1/2. On the contrary, when the plate with q=1/2 is placed first (Fig. 4(d)), the resulting q-plate has the opposite value q=–1/2. As before, the change in the sign is revealed in Fig. 4(d) by the bright areas rotating in the opposite sense as the linear analyzer rotates.

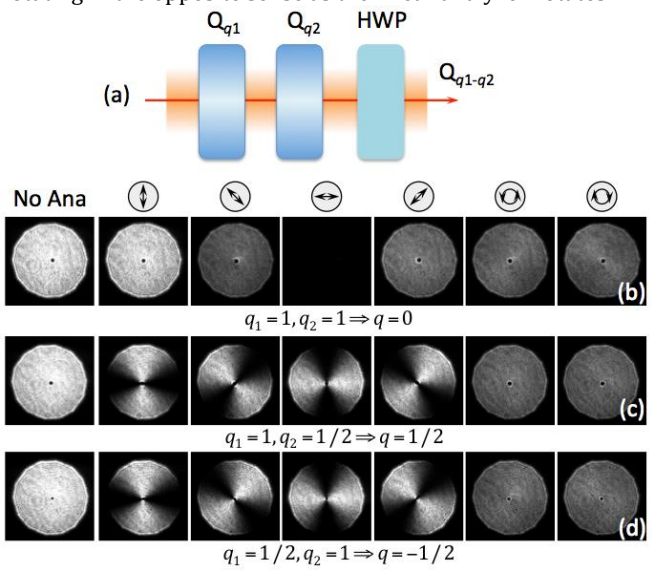

Fig. 4. System for subtracting two q-plates (a) and resulting experimental polarization patterns when illuminated with vertical linear polarization: (b) Subtraction of two q=1 plates; (c) Subtraction of q=1 and q=1/2 plates; (d) Subtraction of q=1/2 and q=1 plates.

4. Full q-spectrum

Finally, using the techniques discussed above, and two q-plates with q=1 and one q-plate with q=1/2, we show ten different combinations where the sum ranges from +5/2 to –5/2 in steps of 1/2, ignoring the null q=0, which is trivial. Table I summarizes the different combinations required to obtain these equivalent q-plate systems. The corresponding experimental results are presented in Fig. 5. For brevity, we only show the results when placing the system between a linear vertical polarizer and a linear analyzer oriented at 45º. The number of bright areas is twice the value of the topological charge generated. In addition, their counterclockwise (or clockwise) rotation indicates the positive (or negative) sign of the q-value. Results agree with theory in all cases.

TABLE I.
Different systems employed to generate equivalent q-plates with different q-values

***q*-value**	**System**
+2.5	$Q_{1/2}$ HWP Q_1 HWP Q_1
+2	Q_1 HWP Q_1
+1.5	$Q_{1/2}$ HWP Q_1
+1	Q_1
+0.5	$Q_{1/2}$
-0.5	HWP $Q_{1/2}$ HWP
-1	HWP Q_1 HWP
-1.5	HWP $Q_{1/2}$ HWP Q_1 HWP
-2	HWP Q_1 HWP Q_1 HWP
-2.5	HWP $Q_{1/2}$ HWP Q_1 HWP Q_1 HWP

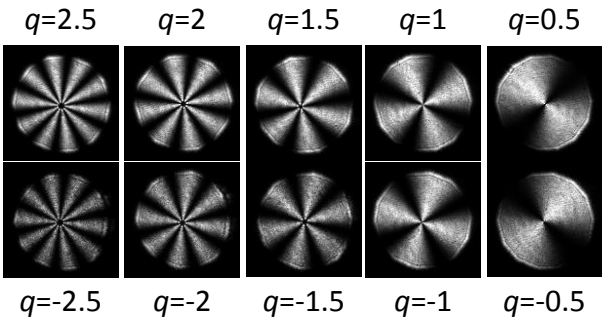

Fig. 5. Polarization pattern results for different effective q-plate systems with q-values ranging from +2.5 to -2.5 in steps of 0.5. Input polarization is always linear vertical, and the analyzer is always linear oriented at 45º.

5. CONCLUSIONS

In conclusion, we have investigated approaches for adding, subtracting, or changing the sign of commercially available q-plates. The approach can be easily implemented in the lab since it only involves the combination of q-plates with half-wave plates. The experimental results clearly show the differences in terms of the charges, whether the charges are positive or negative, and the polarization state that is encoded. In our examples, we obtain ten combinations using only three devices. In general, using three devices with distinct q-values it is possible to obtain 27 combinations, or for an arbitrary number n of distinct q-valued plates it is possible to obtain 3^n combinations. This allows experimental testing of higher or negative q-valued devices without incurring the expense. Consequently, we believe that these results will be of interest to the community.

Funding: MMSL and IM acknowledge financial support from Ministerio de Ciencia e Innovación from Spain (ref. FIS2015-66328-C3-3-R).

References

1. A. M. Yao and M. J. Padgett, "Orbital angular momentum: Origins, behavior and applications", Adv. Opt. Photon. **3**, 161–204 (2011).
2. J. Wang, J.-Y. Yang, I.M. Fazal, N. Ahmed, Y. Yan, H. Huang, Y. Ren, Y. Yue, S. Dolinar, M. Tur, and A.E. Willner, "Terabit free-space data transmission employing orbital angular momentum multiplexing", Nat. Photonics 138, 488 (2012).
3. N. Bozinovic, Y. Yue, Y. Ren, M. Tur, P. Kristensen, H. Huang, A.E. Willner, and S. Ramachandran, "Terabit-scale orbital angular momentum mode division multiplexing in fibers", Science 340, 1545 (2013).
4. T. Lei, M. Zhang, Y. Li, P. Jia, G.N. Liu, X. Xu, Z. Li, C. Min, J. Lin, C. Yu, H. Niu, and X. Yuan, "Massive individual orbital angular momentum channels for multiplexing enabled by Dammann gratings", Light: Science & Applications 4, e257 (2015)
5. G. Milione, M. P. J. Lavery, H. Huang, Y. Ren, G. Xie, T. A. Nguyen, E. Karimi, L. Marrucci, D. A. Nolan, R. R. Alfano, and A. E. Willner, "4×20 Gbit/s mode division multiplexing over free space using vector modes and a q-plate mode (de)multiplexer," Opt. Lett. **40**, 1980-1983 (2015).
6. Q. Zhan, "Cylindrical vector beams: From mathematical concepts to applications," Adv. Opt. Photon. **1**, 1–57 (2009).
7. B. Ndagano, H. Sroor, M. McLaren, C. Rosales-Guzmán, A. Forbes, "Beam quality measure for vector beams", Opt. Lett. **41**, 3407-3410 (2016).
8. S. Quabis, R. Dorn, M. Eberler, O. Glöckl and G. Leuchs, "Focusing light into a tighter spot," Opt. Commun. **179**, 1-7 (2000).
9. R. Dorn, S. Quabis, and G. Leuchs, "Sharper focus for a radially polarized light beams," Phys. Rev. Lett. **91**, 233901 (2003).
10. B. J. Roxworthy, K. C Toussaint Jr, "Optical trapping with π-phase cylindrical vector beams," New. J. Phys. **12**, 073012 (2010).
11. Y. Jin, O. J. Allegre, W. Perrie, K. Abrams, J. Ouyang, E. Fearon, S. P. Edwardson, and G. Dearden, "Dynamic modulation of spatially structured polarization fields for real-time control of ultrafast laser-material interactions," Opt. Express **21**, 25333- 25343 (2013).
12. P. Török and P.R.T. Munro, "The use of Gauss-Laguerre vector beams in STED microscopy," Opt. Express **12**, 3605-3617 (2004).
13. L. Marrucci, C. Manzo, and D. Paparo, "Optical spin-to-orbital angular momentum conversion in inhomogeneous anisotropic media," Phys. Rev. Lett. **96**, 163905 (2006).
14. M. Stalder and M. Schadt, "Linearly polarized light with axial symmetry generated by liquid-crystal polarization converters," Opt. Lett. **21**, 1948-1950 (1996).
15. S. Slussarenko, A. Murauski, T. Du, V. Chigrinov, L. Marrucci, and E. Santamato, "Tunable liquid crystal q-plates with arbitrary topological charge," Opt. Express **19**, 4085-4090 (2011).
16. S. Slussarenko, B. Piccirillo, V. Chigrinov, L. Marrucci, and E. Santamato, "Liquid crystal spatial-mode converters for the orbital angular momentum of light", J. Opt. **15**, 025406 (2013).
17. C. Loussert, K. Kushnir, and E. Brasselet, "Q-plates micro-arrays for parallel processing of the photon orbital angular momentum", Appl. Phys. Lett. **105**, 121108 (2014).
18. A. Niv, Y. Gorodetski, V. Kleiner, and E. Hasman, "Topological spin–orbit interaction of light in anisotropic inhomogeneous subwavelength structures," Opt. Lett. **33**, 2910-2912 (2008).
19. M. Beresna, M. Gecevičius, P. G. Kazansky, and T. Gertus, "Radially polarized optical vortex converter created by femtosecond laser nanostructuring of glass," Appl. Phys. Lett. **98**, 201101 (2011).
20. Y. Liu, X. Ling, X. Yi, X. Zhou, H. Luo, and S. Wen, "Realization of polarization evolution on higher-order Poincaré sphere with metasurface," Appl. Phys. Lett. **104**, 191110 (2014).
21. M. M. Sánchez-López, J. A. Davis, N. Hashimoto, I. Moreno, E. Hurtado, K. Badham, A. Tanabe, and S. W. Delaney, "Performance of a q-plate tunable retarder in reflection for the switchable generation of both first- and second-order vector beams," Opt. Lett. **41**, 13-16 (2016).
22. C. Maurer, A. Jesacher, S. Fürhapter, S. Bernet, and M. Ritsch-Marte, "Tailoring of arbitrary optical vector beams", New J. Phys. 9, 78 (2007).
23. I. Moreno, M. M. Sánchez-López, K. Badham, J. A. Davis, D. M. Cottrell, "Generation of integer and fractional vector beams with q-plates encoded onto a spatial light modulator," Opt. Lett. **41**, 1305-1308 (2016).

24. X. Yi, Y. Li, X. Ling, Y. Liu, Y. Ke, and D. Fan, "Addition and subtraction operation of optical orbital angular momentum with dielectric metasurfaces", Opt. Commun. **356**, 456-462 (2014).
25. X. Yi, X. Ling, Z. Zhang, Y. Li, X. Zhou, Y. Liu, S. Chen, H. Luo, and S. Wen, "Generation of cylindrical vector vortex beams by two cascaded metasurfaces", Opt. Express **22**, 17207-17215 (2014)
26. Y. Li, Y. Liu, X. Ling, X. Yi, X. Zhou, Y. Ke, H. Luo, S. Wen, and D. Fan, "Observation of photonic spin Hall effect with phase singularity at dielectric metasurfaces", Opt. Express **23**, 1767-1774 (2015).
27. J. A. Davis, N. Hashimoto, M. Kurihara, E. Hurtado, M. Pierce, M. M. Sánchez-López, K. Badham, and I. Moreno, "Analysis of a segmented q-plate tunable retarder for the generation of first-order vector beams", Appl. Opt. **54**, 9583-9590 (2015).
28. B. E. A. Saleh and M. C. Teich, Fundamentals of Photonics, John Wiley & Sons (1991).